Clays and Clay Minerals, Vol. 42, No. 2, 148–160, 1994.

THE EFFECT OF DISSOLVED LIGANDS ON THE SORPTION OF Cu(II) BY Ca-MONTMORILLONITE

MARKUS STADLER AND PAUL W. SCHINDLER

Institute for Inorganic Chemistry, University of Berne
Freiestrasse-3, 3012-Berne, Switzerland

Abstract—The effects of three organic ligands on the adsorption of copper on Ca-montmorillonite were studied. The results indicate that these effects include three different processes:

1) Enhanced uptake of positively charged copper-ligand complexes by ion-exchange.
2) Formation of ternary surface complexes involving surface aluminol groups.
3) Inhibited uptake due to competition between the surface ligands and the dissolved ligands for dissolved copper.

Ethylenediamine promotes copper uptake by ion-exchange at low pH but tends to suppress adsorption at aluminol groups by ligand competition at high pH. The same mechanisms are operative for β-alanine; however, the uptake of $Cu(\beta\text{-ala})^+$ by ion-exchange is not promoted by the attached ligand. The influence of malonate includes both ligand competition and formation of ternary complexes. A quantitative interpretation based on the surface complexation model using the least-squares programs FITEQL (Westall, 1982) and GRFIT (Ludwig, 1992) is presented. The obtained equilibrium constants are listed in Tables 2b and 3.

Key Words—Adsorption, β-alanine, Copper, Ethylenediamine, Malonic acid, Modeling, Montmorillonite.

INTRODUCTION

In a previous paper (Stadler and Schindler, 1993), a model of copper adsorption on Ca-montmorillonite was presented. It was found that copper interaction with montmorillonite can be described with a model that contains adsorption of copper by ion-exchange in the interlayers of montmorillonite in the range of $3 < pH < 4.5$ and by the formation of surface complexes with aluminol groups in the region $pH > 4$.

The uptake of metal ions by clay minerals (and oxides) is strongly influenced by the presence of ligands with complexing characteristics. Metal ions in natural systems are in part present as dissolved metal-ligand complexes because of the vast abundance of such ligands. The study of metal uptake by clay minerals in the presence of complexing ligands is, therefore, necessary to understand the fate of metals in soils.

The electrolyte concentration used in this study was significantly higher than that normally found in natural soils. The authors are aware that this choice reduces the relevance of the study to the fate of heavy metals in natural soils. On the other hand, such a high electrolyte concentration offers some important advantages: Activity coefficients of almost all involved components, including surface species and dissolved species, can be neglected, which simplifies the modeling of the investigated systems. Moreover, numerous equilibrium constants in the range of $1.0 > I > 0.1$ (I = ionic strength) for important reactions in this study are present in the literature, which offers a broad and reliable control of the results of this work. Finally, the aim of this study is to give an overview of possible interactions of metals and surface components in the presence of organic ligands and to show the possibilities and limits of least-squares programs in modeling and interpreting complex systems.

The influence of ligands on metal uptake is manifested in different ways. In the simplest case, dissolved ligands compete with the solid phase for the metal cation causing a decreased adsorption of the metal. Ligand competition for metal ions is always occurring, but this decreased adsorption can be compensated by other forms of ligand-metal-solid interactions: The formation of ternary complexes promotes metal adsorption at oxide minerals (Schindler and Stumm, 1987; Schindler, 1990). For clay minerals, an enhanced uptake of cationic metal-ligand complexes by ion-exchange as compared with the free metal ion has been reported (Bodenheimer *et al.*, 1962, 1963, and 1966; Cloos *et al.*, 1972; Maes *et al.*, 1978). This effect was interpreted as a stabilization of the metal-ligand complex by the interlayer phase as compared with the aqueous solution (Maes *et al.*, 1978). The possible formation of ternary surface complexes at clay-water interfaces has so far not been investigated.

In this paper, the clay mineral montmorillonite was chosen because of its variety of adsorption sites. Copper was selected because of its ability to form very stable complexes with different ligands. The ligands used in this study were ethylenediamine (en), β-alanine and malonic acid. β-alanine and malonic acid form six membered chelate rings with copper, which are thought to stabilize copper complexes, whereas en forms a five membered chelate ring.

This work consists of two parts: in the first part, the interactions of montmorillonite with the chosen ligands were investigated. In the second part, the three ternary systems copper-en-montmorillonite, copper-β-alanine-montmorillonite and copper-malonate-montmorillonite were studied. Experimental data were used to establish a model for the investigated systems with the aid of the least-squares fit programs FITEQL (Westall, 1982) and GRFIT (Ludwig, 1992).

MATERIALS AND METHODS

Survey

1.00 g Ca-montmorillonite was suspended in V_0 = 0.1 dm³ of a solution, S, of the general composition $[H^+] = H_0$ mol/dm³, $[Cu_T] = C_0$ mol/dm³, $[L] = L_0$ mol/dm³, $[Ca_T] = (0.1 - C_0)$ mol/dm³, $[ClO_4^-] = 0.2$ mol/dm³ and pre-equilibrated for one week. Afterwards the suspension was titrated at 298.2 K with v dm³ of a solution, S1, of the general composition $[Ca^{2+}]$ = 0.1 mol/dm³, $[OH^-] = B$ mol/dm³, $[ClO_4^-] = (0.2 - B)$ mol/dm³. H_0 was set close to 0.002 mol/dm³; L_0 was varied in the range of $0.0001 \leq L_0 \leq 0.0040$ mol/dm³; and B was set at 0.01 mol/dm³. In most of the titrations, C_0 was 0.0005 mol/dm³.

Separate titrations with $C_0 = 0$ mol/dm³ were carried out to investigate ligand uptake by Ca-montmorillonite. After each addition of S1, the free concentration of hydrogen ions was measured every 30 s with the aid of a combined glass electrode. Equilibrium was assumed when 1) two consecutive readings of the emf E_H differed less than 0.01 mV and 2) a given reading did not differ more than 0.05 mV from the average of the six foregoing readings. When the equilibrium was established, a small aliquot was collected and analyzed after centrifugation for both dissolved copper (C_s) and ligand (L_s).

The following parameters are thus accessible: Total hydrogen ion concentration, H, is given by

$$H = \frac{H_0 \cdot V_0 - B \cdot v}{V_0 + v} \quad (1)$$

Free hydrogen ion concentration, h, is obtained from the Nernst equation:

$$h = 10^{\frac{E_H - E_H^0}{k}} \quad (2)$$

E_H^0 and k were obtained from calibrations using a series of solutions with known H^+-concentration. Total copper concentration, C, and total ligand concentration, L, are calculated with Eqs. 3 and 4, respectively:

$$C = \frac{C_0 \cdot V_0}{V_0 + v} \quad (3)$$

$$L = \frac{L_0 \cdot V_0}{V_0 + v} \quad (4)$$

Table 1. Layer distances of montmorillonite.

	d [Å]	Ref.
Ca-montmorillonite	14.5	Stadler and Schindler, 1993
Ca-en-montmorillonite	15.2	This work
Cu-montmorillonite	12	Stadler and Schindler, 1993
Cu-en-montmorillonite	15.5	This work

The amount of adsorbed copper and ligand respectively is given by:

$$C_{ads} = C - C_s \quad (5)$$

$$L_{ads} = L - L_s \quad (6)$$

Experimental and calculated data are presented in the Figures as:

$$\Delta C = \frac{C_{ads}}{C} \cdot 100\ [\%] \quad (5a)$$

$$\Delta L = \frac{L_{ads}}{L} \cdot 100\ [\%] \quad (6a)$$

Chemicals

SWy-1 montmorillonite (Na-montmorillonite) from Crook County, Wyoming, was provided by the Clay Minerals Society. Ca-montmorillonite was prepared as described in Stadler and Schindler (1993). d_{001} spacings of Ca-montmorillonite as well as of other forms of montmorillonite were obtained from X-ray diffraction (Cu kα radiation) and are given in Table 1.

Solutions of $HClO_4$, $Ca(ClO_4)_2$, $Ca(OH)_2$, and $Cu(ClO_4)_2$ were prepared and analyzed as described in Stadler and Schindler (1993).

^{14}C-labeled ethylenediamine (purity ≥97.1%) and ^{14}C-labeled malonate (sodium salt, purity 98.9%) were provided by Amersham International. ^{14}C-labeled β-alanine (purity >98%) was obtained from Sigma. Diluted solutions with an activity close to 10 kBq per mmol of ligand (L) were prepared by mixing labeled L with 0.1 mol/dm³ solutions of unlabeled ethylenediamine (Merck p.a.), β-alanine (Merck p.a.), and malonic acid (Merck p.a.), respectively. The activities of these solutions were regularly checked. Opti-Fluor (Packard Instrument Company) was used as liquid scintillation cocktail.

Apparatus

The titration equipment used in this work and the procedure for calibrating the glass electrode have been described by Stadler and Schindler (1993). Centrifugation was carried out for five min at 2500 rpm. C_s was obtained from flame-AAS (Beckmann AAS 1248); L_s was determined with the aid of a scintillation counter (Kontron Betamatic Isc).

https://doi.org/10.1346/CCMN.1994.0420205 Published online by Cambridge University Press

Table 2a. Equilibria with fixed stability constants (I (ionic strength) = 0.3, 298.2 K).

Equilibrium	log K
$H_2O \Leftrightarrow H^+ + OH^-$	−13.76[1]
$Ca^{2+} (+ H_2O) \Leftrightarrow CaOH^+ + H^+$	−11.58[2]
$en + H^+ \Leftrightarrow (en)H^+$	+9.96[3]
$en + 2H^+ \Leftrightarrow (en)H_2^{2+}$	+17.16[3]
$\beta\text{-ala}^- + H^+ \Leftrightarrow (\beta\text{-ala})H$	+10.07[4]
$\beta\text{-ala}^- + 2H^+ \Leftrightarrow (\beta\text{-ala})H_2^+$	+13.58[4]
$mal^{2-} + H^+ \Leftrightarrow (mal)H^-$	+5.23[4]
$mal^{2-} + 2H^+ \Leftrightarrow (mal)H_2$	+7.85[4]
$mal^{2-} + Ca^{2+} \Leftrightarrow Ca(mal)$	+1.40[4]
$2X^- + Ca^{2+} \Leftrightarrow CaX_2$	+20.00[2]
$2X^- + Cu^{2+} \Leftrightarrow CuX_2$	+20.30[2]
$\equiv SOH + H^+ \Leftrightarrow \equiv SOH_2^+$	+8.16[2]
$\equiv SOH - H^+ \Leftrightarrow \equiv SO^-$	−8.71[2]
$\equiv TOH - H^+ \Leftrightarrow \equiv TO^-$	−5.77[2]
$\equiv SOH + Cu^{2+} \Leftrightarrow \equiv SOHCu^{2+}$	+5.87[2]
$\equiv SOH - H^+ + Cu^{2+} \Leftrightarrow \equiv SOCu^+$	−0.57[2]
$\equiv SOH - 2H^+ + Cu^{2+} \Leftrightarrow \equiv SOCuOH$	−6.76[2]

[1] Sillèn and Martell (1964).
[2] Stadler and Schindler (1993).
[3] Martell and Smith (1976); the value was obtained by interpolating the stability constants given for I = 0.1 and I = 0.5 (T = 298.2 K).
[4] Martell and Smith (1976); calculated from the value given for I = 0.1 (T = 298.2 K) with the aid of the Davies equation.

Table 2b. Equilibria with optimized stability constants (I = 0.3, T = 298.2 K).

Equilibrium	log K
$en + Cu^{2+} \Leftrightarrow Cu(en)^{2+}$	+11.20
$2en + Cu^{2+} \Leftrightarrow Cu(en)_2^{2+}$	+20.59
$\beta\text{-ala}^- + Cu^{2+} \Leftrightarrow Cu(\beta\text{-ala})^+$	+8.32
$2\beta\text{-ala}^- + Cu^{2+} \Leftrightarrow Cu(\beta\text{-ala})_2$	+13.86
$mal^{2-} + Cu^{2+} \Leftrightarrow Cu(mal)$	+4.94
$2mal^{2-} + Cu^{2+} \Leftrightarrow Cu(mal)_2^{2-}$	+9.06

DATA TREATMENT

The model of the H^+ and Cu^{2+} sorption on Ca-montmorillonite as presented in Stadler and Schindler (1993) was extended to the ligands studied in this work. The complete system, therefore, can be described as having seven components: H^+, Cu^{2+}, Ca^{2+}, X^- (ion-exchanger species), ≡SOH (aluminol groups), ≡TOH (silanol groups) and L[ethylenediamine (en), and β-alanine (β-ala) and malonate (mal)].

A reduced system without copper was chosen to study the interactions of the ligands with montmorillonite.

In speciation calculations, it was found that copper hydrolysis for $C \leq 0.0005$ mol/dm³ is negligible in the presence of the strongly complexing ligands en, β-ala, and mal. Furthermore, it was found in various test runs that the inclusion of silanol groups (≡TOH) was not critical to the fit of the different models presented in this study. The same results were obtained for the copper adsorption on montmorillonite (Stadler and Schindler, 1993).

The studied systems, therefore, include known equilibria (Tables 2a and 2b) and the interactions of en, β-ala and mal, respectively, with clay components. The stability constants of most of the equilibria used in this investigation could be derived from published values (Table 2a); however, some solution equilibria for which the pertinent equilibrium constants for the ionic medium used in this study could not be derived from published values were included in the optimization procedure described below. The obtained values are given in Table 2b. With regard to the very different properties of the individual ligands, it is not possible to summarize the different equilibria encountered in the course of this study by one general equation. Therefore, the equilibria considered in modeling the experimental data are defined separately for every ligand in the respective section.

Modeling was performed with the least-squares programs FITEQL (Westall, 1982) and GRFIT (Ludwig, 1992), respectively. The latter program permits a graphical comparison of experimental and calculated data.

RESULTS AND DISCUSSION

The binary system Ca-montmorillonite-en (ethylenediamine)

The choice of ethylenediamine instead of 1,3 diaminopropane, which forms a six membered chelate ring (as β-alanine and malonic acid do), was imposed by the problems encountered in estimating the concentration of dissolved ligand in the montmorillonite suspensions. Since the envisaged ligands do not possess chromophores that permit their determination by UV/VIS spectrometry, we were limited to ligands where ^{14}C-labeled samples were commercially available and labeled 1,3 diaminopropane was not available.

In the measured range of $3 \leq -\log h \leq 8$, en forms protonated and, thus, positively charged species that can undergo ion-exchange. In Figure 1A, the percentage of bound en is plotted against −log h. The figure includes data with $0.0001 \leq L_0 \leq 0.001$ mol/dm³. With regard to the high Ca:en ratio, a maximum of about 3% of the ion-exchange capacity has been occupied by protonated en. The formal treatment of the pertinent ion-exchange reactions as required by FITEQL is described by the hypothetical equilibria (7)–(9), where the value for log K_0 (Eq. 7) was arbitrarily chosen according to the data treatmnt of the ion-exchange as presented by Stadler and Schindler (1993), which is based on the treatment of ion-exchange reactions presented by Shaviv *et al.* (1985) and Fletcher *et al.* (1989).

$$2\,X^- + Ca^{2+} \Leftrightarrow CaX_2$$

$$K_0 = \frac{[CaX_2]}{[Ca^{2+}] - [X^-]^2} = 10^{+20} \quad (7)$$

https://doi.org/10.1346/CCMN.1994.0420205 Published online by Cambridge University Press

$$X^- + en + H^+ \Leftrightarrow (enH)X$$

$$K_8 = \frac{[(enH)X]}{[en]\cdot[H^+]\cdot[X^-]} \quad (8)$$

$$2X^- + en + 2H^+ \Leftrightarrow (enH_2)X_2$$

$$K_9 = \frac{[(enH_2)X_2]}{[en]\cdot[H^+]^2\cdot[X^-]^2} \quad (9)$$

Resulting constants are collected in Table 3. Combining Eqs. 7–9 with:

$$en + H^+ \Leftrightarrow enH^+$$

$$K_{10} = \frac{[enH]}{[en]\cdot[H^+]} \quad (10)$$

$$en + 2H^+ \Leftrightarrow enH_2^{2+}$$

$$K_{11} = \frac{[enH_2]}{[en]\cdot[H^+]^2} \quad (11)$$

one obtains the two ion-exchange constants $K_{ex,Ca,enH}$ and K_{ex,Ca,enH_2}:

$$K_{ex,Ca,enH} = \frac{[(enH)X]^2\cdot[Ca^{2+}]}{[CaX_2]\cdot[enH^+]^2}$$

$$= \frac{K_8^2}{K_{10}^2\cdot K_0} = 10^{-0.36} \quad (12)$$

$$K_{ex,Ca,enH_2} = \frac{[(enH_2)X_2]\cdot[Ca^{2+}]}{[CaX_2]\cdot[enH_2^{2+}]}$$

$$= \frac{K_9}{K_{11}\cdot K_0} = 10^{+0.63} \quad (13)$$

We note that the calculated value of log $K_{ex,Ca,enH}$ is close to reported values for divalent-monovalent ion-exchange. For the exchange reaction $Ca^{2+} \Leftrightarrow Na^+$, an exchange constant of log $K_{ex} = -0.198$ is published (Benson, 1982). The constant of the exchange of Ca^{2+} by enH_2^{2+} is comparatively high and indicates significant preference of the ion-exchanger for enH_2^{2+} as

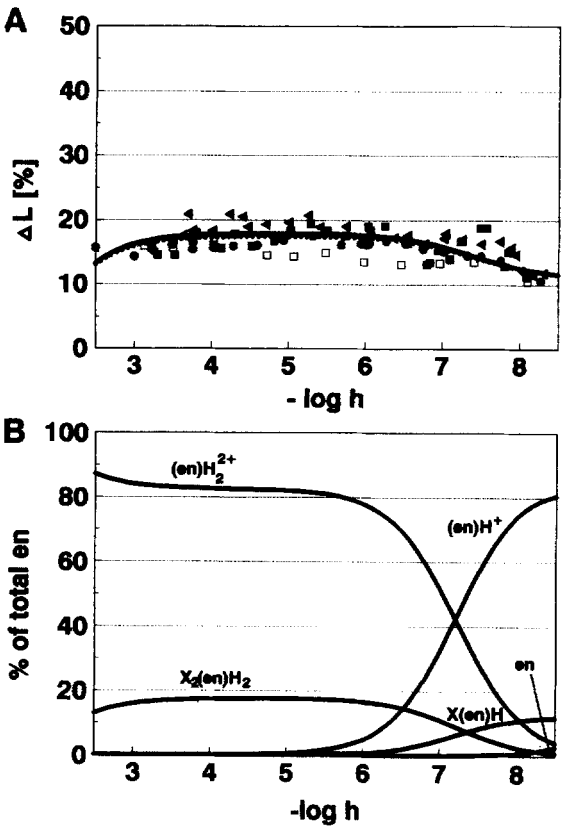

Figure 1. A) Adsorption of en on Ca-montmorillonite. The percentage of adsorbed en, ΔL, is plotted as a function of −log h (I = 0.3, T = 298.2 K). Symbols indicate experimental values for L_0 = 0.0001 mol/dm³ (●), L_0 = 0.0002 mol/dm³ (▲), L_0 = 0.0005 mol/dm³ (■), L_0 = 0.0010 mol/dm³ (□). Lines indicate calculated curves for L_0 = 0.0001 mol/dm³ (——), L_0 = 0.0002 mol/dm³ (- - - -), L_0 = 0.0005 mol/dm³ (· · · · ·), and L_0 = 0.0010 mol/dm³ (- · - · ·). The curves were calculated with the stability constants given in Tables 2a and 3. B) Speciation of en in the system H^+, Ca-montmorillonite, en. The species are plotted in % of L_0 = (total en) against −log h for L_0 = 0.0001 mol/dm³. Calculations were performed with GRFIT (Ludwig, 1992) based on the values given in Tables 2a and 3.

Table 3. Equilibria of clay-ligand(-copper) complexes obtained in this study (I = 0.3, T = 298.2 K).

Equilibrium	Stability constant
$X^- + en + H^+ \Leftrightarrow (enH)X$	log K_8 = +19.78 (±0.06)*
$2X^- + en + 2H^+ \Leftrightarrow (enH_2)X_2$	log K_9 = +37.79 (±0.21)*
$2X^- + en + Cu^{2+} \Leftrightarrow Cu(en)X_2$	log K_{17} = +32.28**
$2X^- + 2en + Cu^{2+} \Leftrightarrow Cu(en)_2X_2$	log K_{18} = +42.41**
$2X^- + 3en + Cu^{2+} \Leftrightarrow Cu(en)_3X_2$	log K_{19} = +49.42**
$\equiv SOH + en + Cu^{2+} \Leftrightarrow \equiv SOHCu(en)^{2+}$	log K_{22} = +16.06**
$\equiv Y + \beta\text{-ala}^- + H^+ \Leftrightarrow \equiv Y(\beta\text{-ala})H$	log K_{14} = +14.60 (±0.10)*
$X^- + Cu^{2+} + \beta\text{-ala}^- \Leftrightarrow Cu(\beta\text{-ala})X$	log K_{30} = +18.27**
$\equiv SOH + mal^{2-} + 2H^+ \Leftrightarrow \equiv SOH_2(mal)H$	log K_{15} = +15.63 (±0.03)*
$\equiv SOH + mal^{2-} + H^+ \Leftrightarrow \equiv SOH_2(mal)^-$	log K_{16} = +10.86 (±0.03)*
$\equiv SOH + Cu^{2+} + mal^{2-} \Leftrightarrow \equiv SOCu(mal)^- + H^+$	log K_{32} = +3.12**
$\equiv SOH + Cu^{2+} + mal^{2-} \Leftrightarrow \equiv SOHCu(mal)$	log K_{33} = +9.34**

* 3 σ.

** Constants obtained from GRFIT; the present version gives no estimation of the standard deviation.

https://doi.org/10.1346/CCMN.1994.0420205 Published online by Cambridge University Press

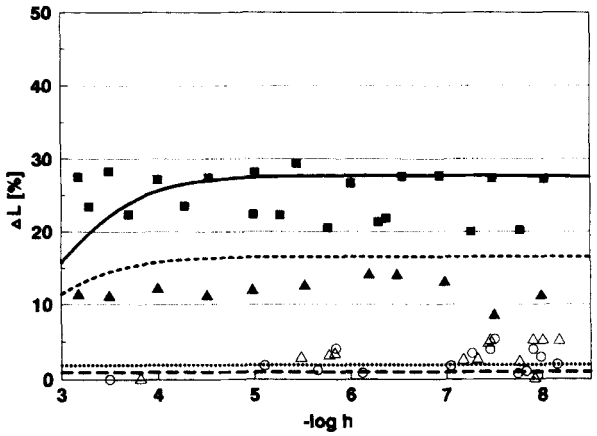

Figure 2. Sorption of β-alanine on Ca-montmorillonite (I = 0.3, T = 298.2 K). ΔL, the percentage of β-ala sorbed, is plotted against $-\log h$. Symbols indicate experimental data for $L_0 = 0.0001$ mol/dm^3 (■), $L_0 = 0.0002$ mol/dm^3 (▲), $L_0 = 0.0020$ mol/dm^3 (△), $L_0 = 0.0040$ mol/dm^3 (○). Lines indicate calculated curves for $L_0 = 0.0001$ mol/dm^3 (——), $L_0 = 0.0002$ mol/dm^3 (- - - - -), $L_0 = 0.0020$ mol/dm^3 (· · · · ·), and $L_0 = 0.0040$ mol/dm^3 (– – –). The curves were calculated with the stability constants given in Tables 2a and 3.

compared with Ca^{2+}. As seen from the diagram (Figure 1B), the modeled speciation in the ion-exchanger phase closely reflects the speciation in solution. Uptake of enH^+ and enH_2^{2+} to form interlayer complexes has already been investigated in an IR study by Cloos *et al.* (1972). These authors report a d_{001} spacing of 12.2 Å for the pure en form. In this work, only a partial exchange of Ca^{2+} by enH_2^{2+} of $\leq 3\%$ of the total exchange capacity was investigated. The d_{001} spacing of Ca-montmorillonite was, thus, not significantly changed by the uptake of the small amount of enH_x^{x+}.

The system Ca-montmorillonite-β-alanine

Experimental data of β-alanine sorption by Ca-montmorillonite are shown in Figure 2. The total amount of β-ala sorbed on the surface ($\approx 2.5 \cdot 10^{-5}$ mol/dm^3) does neither change with log h (in the range of $3 < -\log h < 8$) nor with increasing L_0 concentrations varying from 0.0001 mol/dm^3 to 0.004 mol/dm^3. This behavior could not be explained within the existing set of components. Therefore, an additional component $\equiv Y$ ($[\equiv Y]_{tot} = 4.0 \cdot 10^{-5}$ mol/dm^3) was introduced. It must be emphasized that the presence of $\equiv Y$ in the model is purely empirical and cannot be taken as evidence for the existence of such hydrophobic sites. The equilibrium:

$$K_{14} = \frac{[\equiv Y(\beta\text{-ala})H]}{[\equiv Y] \cdot [\beta\text{-ala}^-] \cdot [H^+]} \qquad (14)$$

serves merely to formally account for the observed unspecific, perhaps zero-order sorption within the scope of the FITEQL concept. This unsatisfactory handling of the experimental data in the case of β-alanine shows clearly the limits of the available least-squares programs in fitting systems with complex and probably not exclusively chemical interactions. However, with respect to the ternary system copper-β-alanine-montmorillonite, this doubtful model-fitting treatment was not excluded from this study.

The parameters obtained by the optimization procedure are listed in Table 3, the modeled curve is plotted in Figure 2. According to Tsunashima (1984), the protonated β-alanine undergoes ion-exchange with Ca-montmorillonite at $-\log h < 4$. In the present study, this ion-exchange was obviously suppressed by the prevailing high concentration of Ca^{2+} ions.

Adsorption of malonate and hydrogen-malonate on Ca-montmorillonite

The uptake of malonate by Ca-montmorillonite is shown in Figure 3A. Adsorption occurs preferentially under moderate acidic conditions with a maximum at $-\log h = 4.5$ and becomes negligible at $-\log h > 8$. Similar behavior is widely observed with anionic species that undergo electrostatic interactions with a positively charged surface. The speciation of L in the measured log h range ($3 < -\log h < 8$) is governed by the anions mal^{2-} and $(mal)H^-$. For electrostatical reasons, the interaction of the ligand with montmorillonite is likely to take place at positively charged aluminol surface sites (Siffert *et al.*, 1980). Therefore, all models tested in this study included complexes of $(mal)H^-$ and mal^{2-} with protonated aluminol-groups.

The best fit was obtained with a combination of the two surface complexes $\equiv SOH_2(mal)H$ and $\equiv SOH_2(mal)^-$:

$$\equiv SOH + mal^{2-} + 2H^+ \leftrightarrow \equiv SOH_2(mal)H$$

$$K_{15} = \frac{[\equiv SOH_2(mal)H]}{[\equiv SOH] \cdot [mal^{2-}] \cdot [H^+]^2} \qquad (15)$$

$$\equiv SOH + mal^{2-} + H^+ \leftrightarrow \equiv SOH_2(mal)^-$$

$$K_{16} = \frac{[\equiv SOH_2(mal)^-]}{[\equiv SOH] \cdot [mal^{2-}] \cdot [H^+]} \qquad (16)$$

The obtained equilibrium constants are presented in Table 3.

The model is able to explain the adsorption properties of malonic acid in the whole log h range measured in this study: As seen from Figure 3B, the speciation of L at $-\log h \leq 3.0$ is dominated by malonic acid ($H_2(mal)$) that is not able to interact with the positively charged aluminol sites. In the range of $3 < -\log h < 4$, L is predominantly present as $(mal)H^-$ and $\equiv SOH_2(mal)H$, respectively. In the subsequent log h range ($4 < -\log h < 5.5$), a slight decrease of ΔL is observed in the same region as $(mal)H^-$ is transformed into mal^{2-}. The decrease in ΔL becomes steeper at values of $-\log h > 5.5$ due to the beginning depro-

tonation of surface aluminol groups. At $-\log h > 8$, L is completely desorbed.

The structure of the aluminol-malonate complex is not directly accessible with the methods used in this study. The obtained stability constants are, however, more in accordance with an outer sphere complex (I) than with an inner sphere complex based on ligand exchange (II):

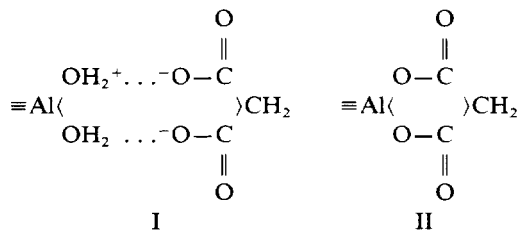

Combining

$$\equiv SOH_2^+ \Leftrightarrow \equiv SOH + H^+$$

$$\log K = -8.16$$

$$\equiv SOH + mal^{2-} + H^+ \Leftrightarrow \equiv SOH_2(mal)^-$$

$$\log K_{16} = 10.86$$

one obtains the equilibrium:

$$\equiv SOH_2^+ + mal^{2-} \Leftrightarrow \equiv SOH_2(mal)^- \quad \log K = 2.70$$

This is markedly smaller than what one would expect for the formation constant of Al(III)-malonate complex in solution,

$$Al_{aq}^{3+} + mal^{2-} \Leftrightarrow Al(mal)^+$$

on the basis of published values for $Sc(mal)^+$ ($\log K = 5.87$, 298.2 K, I = 1 (Martell and Smith, 1976) and $Fe(mal)^+$ ($\log K = 7.5$, 298.2 K, I = 1 (Martell and Smith, 1976)). On the other hand, the observation that the protonation constant as obtained from Eqs. 15 and 16:

$$\equiv SOH_2(mal)^- + H^+ \Leftrightarrow \equiv SOH_2(mal)H$$

$$\log K^s = 4.77$$

is smaller than the protonation constant of malonate in solution:

$$mal^{2-} + H^+ \Leftrightarrow (mal)H^- \quad \log K^s = 5.26$$

is in accordance with the formation of an outer sphere complex (I) and reflects the presence of the neighboring positive surface charge.

The ternary system ethylenediamine-copper-Ca-montmorillonite

Collected data for en and copper adsorption are plotted in Figures 4A and 4B, respectively.

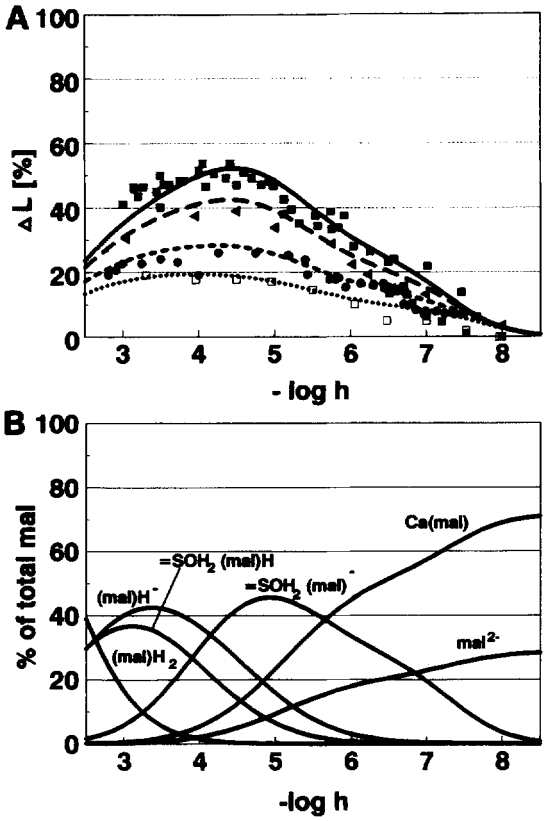

Figure 3. A) Sorption of mal on Ca-montmorillonite (I = 0.3, T = 298.2 K). The percentage of adsorbed ligand, ΔL, is plotted against $-\log h$. Symbols indicate experimental data for $L_0 = 0.0001$ mol/dm³ (■), $L_0 = 0.0002$ mol/dm³ (▲), $L_0 = 0.0005$ mol/dm³ (●) and $L_0 = 0.0010$ mol/dm³ (□). Lines indicate calculated curves for $L_0 = 0.0001$ mol/dm³ (——), $L_0 = 0.0002$ mol/dm³ (– – –), $L_0 = 0.0005$ mol/dm³ (-----), and $L_0 = 0.0010$ mol/dm³ (· · · · ·). The curves were calculated with the stability constants given in Tables 2a and 3. B) Speciation of mal in the system H^+, Ca-montmorillonite, mal. The species are plotted in % of L_0 (total mal) *vs.* $-\log h$. Calculations were performed with the aid of GRFIT (Ludwig, 1992) for $L_0 = 0.0001$ mol/dm³.

The system is clearly dominated by two processes. Those include 1) The formation of very stable Cu-en complexes in solution (the formation of $Cu(en)^{2+}$ and $Cu(en)_2^{2+}$ is well documented, while the formation of a $Cu(en)_3^{2+}$-complex is uncertain); and 2) uptake of copper-en complexes by the interlayers of montmorillonite. The adsorption of $Cu(en)_2^{2+}$ by ion-exchange has already been described by Bodenheimer *et al.* (1963). Velghe *et al.* (1977) report the formation of $Cu(en)^{2+}$, $Cu(en)_2^{2+}$ and $Cu(en)_3^{2+}$ in the interlayer space. Maes *et al.* (1978) found a markedly enhanced stability of $Cu(en)^{2+}$ and $Cu(en)_2^{2+}$ in the interlayer as compared with the stability in solution.

Therefore, the combined copper-en uptake by montmorillonite can be described by the equilibria:

$$2X^- + Cu^{2+} + en \Leftrightarrow (Cu(en))X_2$$

https://doi.org/10.1346/CCMN.1994.0420205 Published online by Cambridge University Press

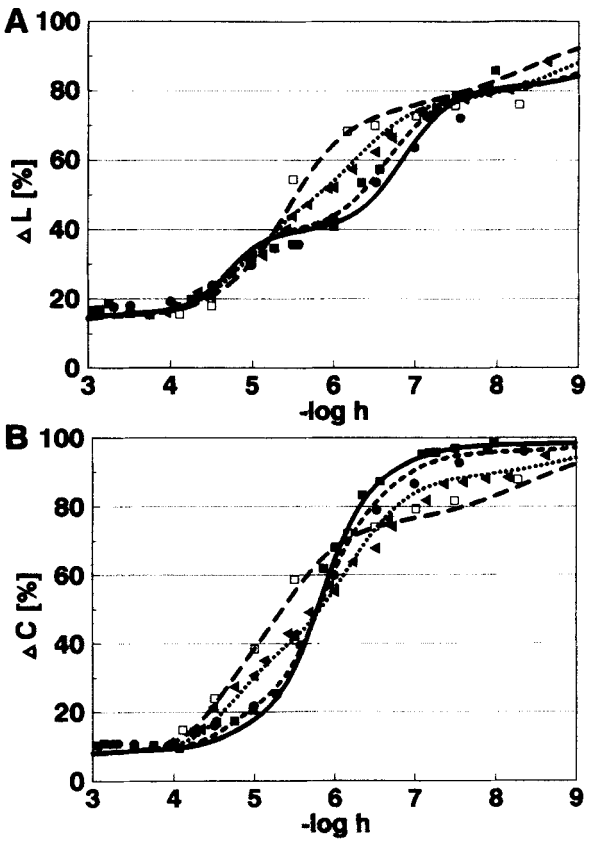

Figure 4. A) Adsorption of en on Ca-montmorillonite in the presence of Cu(II) (C_0 = 0.0005 mol/dm³, I = 0.3, T = 298.2 K). The percentage of adsorbed en, ΔL, is plotted as a function of −log h. Symbols denote experimental values for L_0 = 0.0001 mol/dm³ (■), L_0 = 0.0002 mol/dm³ (●), L_0 = 0.0005 mol/dm³ (▲), L_0 = 0.0010 mol/dm³ (□). Lines indicate calculated curves for L_0 = 0.0001 mol/dm³ (——), L_0 = 0.0002 mol/dm³ (-----), L_0 = 0.0005 mol/dm³ (· · · · ·), and L_0 = 0.0010 mol/dm³ (– – –). The curves were calculated with the stability constants given in Tables 2 and 3. B) Adsorption of Cu(II) on Ca-montmorillonite in the presence of en. (C_0 = 0.0005 mol/dm³, I = 0.3, T = 298.2 K). The percentage of adsorbed Cu(II), ΔC is plotted against −log h. Symbols indicate experimental values for L_0 = 0.0001 mol/dm³ (■), L_0 = 0.0002 mol/dm³ (●), L_0 = 0.0005 mol/dm³ (▲), L_0 = 0.0010 mol/dm³ (□). Lines indicate calculated curves for L_0 = 0.0001 mol/dm³ (——), L_0 = 0.0002 mol/dm³ (-----), L_0 = 0.0005 mol/dm³ (· · · · ·), and L_0 = 0.0010 mol/dm³ (– – –). The curves were calculated with the stability constants given in Tables 2 and 3.

$$K_{17} = \frac{[(Cu(en))X_2]}{[Cu^{2+}]\cdot[en]\cdot[X^-]^2} \quad (17)$$

$$2X^- + Cu^{2+} + 2\ en \Leftrightarrow (Cu(en)_2)X_2$$

$$K_{18} = \frac{[(Cu(en)_2)X_2]}{[Cu^{2+}]\cdot[en]^2\cdot[X^-]^2} \quad (18)$$

$$2X^- + Cu^{2+} + 3\ en \Leftrightarrow (Cu(en)_3)X_2$$

$$K_{19} = \frac{[(Cu(en)_3)X_2]}{[Cu^{2+}]\cdot[en]^3\cdot[X^-]^2} \quad (19)$$

In addition, the subsequent equilibria were included in the optimization procedure:

$$Cu^{2+} + en \Leftrightarrow Cu(en)^{2+}$$

$$K_{20} = \frac{[Cu(en)^{2+}]}{[Cu^{2+}]\cdot[en]} \quad (20)$$

$$Cu^{2+} + 2\ en \Leftrightarrow Cu(en)_2{}^{2+}$$

$$K_{21} = \frac{[Cu(en)_2{}^{2+}]}{[Cu^{2+}]\cdot[en]^2} \quad (21)$$

The model curves calculated from the above constants are already in good agreement with the experimental data. A slight improvement was achieved introducing the ternary surface complex ≡SOHCu(en)²⁺ as defined by Eq. 22.

$$\equiv SOH + Cu^{2+} + en \Leftrightarrow \equiv SOHCu(en)^{2+}$$

$$K_{22} = \frac{[\equiv SOHCu(en)^{2+}]}{[Cu^{2+}]\cdot[en]\cdot[\equiv SOH]} \quad (22)$$

Resulting adsorption curves for en and Cu^{2+} are shown in Figures 4A and 4B, respectively; the constants are presented in Tables 2b and 3.

Combining Eqs. 17–18 and 20–21 with Eq. 7 yields the equilibrium constants for the ion-exchange reactions with Ca^{2+}:

$$K_{ex,Ca,Cu(en)} = \frac{[Cu(en)X_2]\cdot[Ca^{2+}]}{[Cu(en)^{2+}]\cdot[CaX_2]}$$

$$= \frac{K_{17}}{K_{20}\cdot K_0} = 10^{1.08} \quad (23)$$

$$K_{ex,Ca,Cu(en)2} = \frac{[Cu(en)_2X_2]\cdot[Ca^{2+}]}{[Cu(en)_2{}^{2+}]\cdot[CaX_2]}$$

$$= \frac{K_{18}}{K_{21}\cdot K_0} = 10^{1.82} \quad (24)$$

Maes *et al.* (1978) published log K values for the reactions:

$$X_2Cu + en \Leftrightarrow X_2Cu(en)$$

$$K_{25} = \frac{[Cu(en)X_2]}{[CuX_2]\cdot[en]} = 10^{+11.60} \quad (25)$$

$$X_2Cu + 2\ en \Leftrightarrow X_2Cu(en)_2$$

$$K_{26} = \frac{[Cu(en)_2X_2]}{[CuX_2]\cdot[en]^2} = 10^{+23.10} \quad (26)$$

In order to facilitate the comparison of the results of this study with the data published by Maes *et al.* (1978), the equilibria 17 and 18 are combined with the uptake of copper by the ion-exchanger as defined by Stadler and Schindler (1993):

https://doi.org/10.1346/CCMN.1994.0420205 Published online by Cambridge University Press

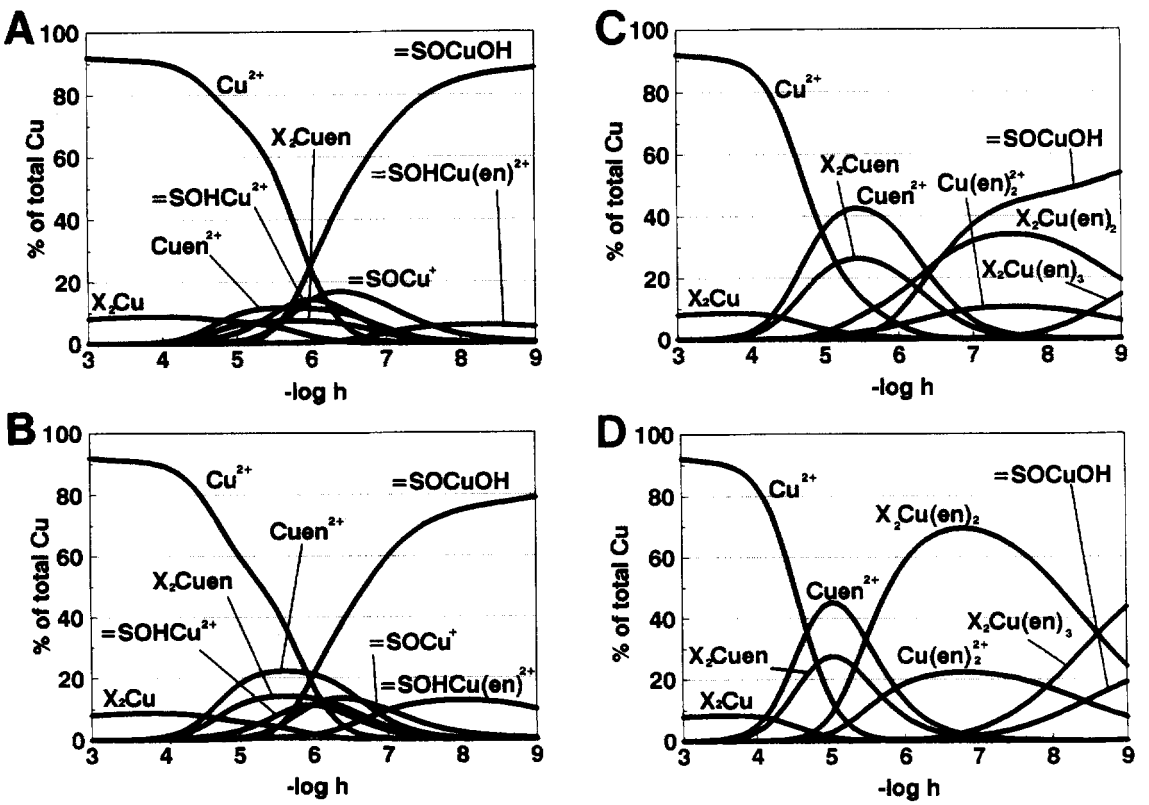

Figure 5. Speciation of Cu(II) in the system H^+, Ca-montmorillonite, en, Cu(II). The species are plotted in % of C_0 (total Cu(II)) *vs.* −log h. Calculations were performed with the aid of GRFIT (Ludwig, 1992) for A) L_0 = 0.0001 mol/dm³, B) L_0 = 0.0002 mol/dm³, C) L_0 = 0.0005 mol/dm³, and D) L_0 = 0.0010 mol/dm³. C_0 was held constant at 0.0005 mol/dm³.

$$2\,X^- + Cu^{2+} \Leftrightarrow X_2Cu$$

$$K_{27} = \frac{[CuX_2]}{[Cu^{2+}]\cdot[X^-]^2} = 10^{+20.30} \quad (27)$$

Dividing Eqs. 17 and 18, respectively, by Eq. 27 yields the equilibrium constants for the reaction 25 and 26. As can be seen, the resulting value of $10^{+11.98}$ for K_{25} is higher than the one published by Maes *et al.* (1978) by a factor of 2.4, whereas the obtained value of $10^{+22.11}$ for K_{26} is markedly lower than the one published by Maes *et al.* (1978).

When the difference log K_{25} − log K_{20} and log K_{26} − log K_{21} is caculated, a stabilization factor of 6.0 for the 1:1 copper-en complex and 32.36 for the 1:2 copper-en complex, respectively, is obtained. Maes *et al.* (1978) found a stabilization factor for the 1:2 complex in the range of 850–1250.

As already mentioned, the formation of $Cu(en)_3^{2+}$ in solution is not well established and the species was, thus, not included in the model. The only published value for this complex (Bjerrum, 1948) seems to indicate that the tendency to attach a third ligand according to:

$$Cu(en)_2^{2+} + en \Leftrightarrow Cu(en)_3^{2+}$$

$$K_{28} = \frac{[Cu(en)_3^{2+}]}{[Cu(en)_2^{2+}]\cdot[en]} = 10^{-0.9} \quad (28)$$

is very low. On the other hand, the stability constant that characterizes the uptake of a third ligand molecule by $X_2Cu(en)_2$ as obtained from Eqs. 18 and 19:

$$K_{29} = \frac{[Cu(en)_3X_2]}{[Cu(en)_2X_2]\cdot[en]} = \frac{K_{19}}{K_{18}} = 10^{+7.01} \quad (29)$$

is amazingly high. The reliability of this value is questionable since the sensitivity of the model to the introduction of $Cu(en)_3X_2$ into the calculations is comparatively modest.

The stability constant of the ternary complex $\equiv SOHCu(en)^{2+}$ as defined by Eq. 22 was found to be very near a value expected from statistical considerations (Schindler, 1990). These considerations predict for the quotient:

$$Q_1 = \frac{K^s_{\equiv SOHCu^{2+}}}{K^s_{\equiv SOHCu(en)^+}}$$

a value of 12 for the case that the structure of the complex can be visualized by

https://doi.org/10.1346/CCMN.1994.0420205 Published online by Cambridge University Press

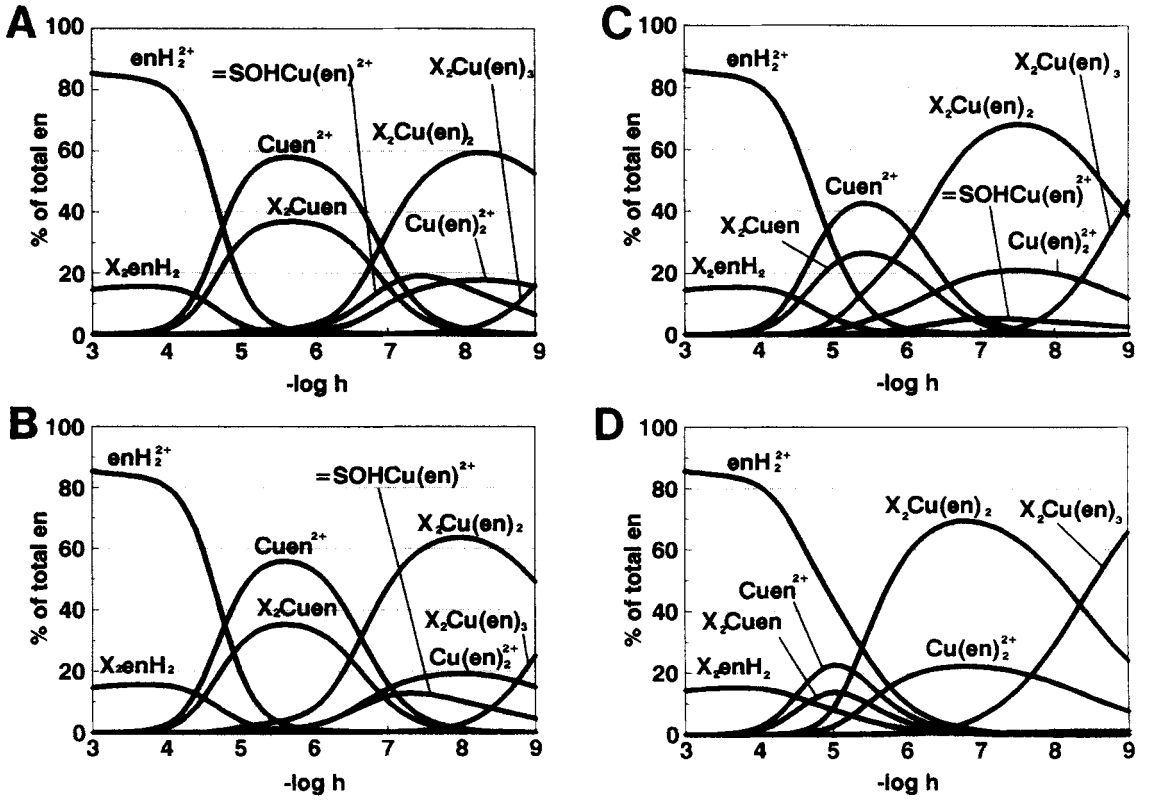

Figure 6. Speciation of en in the system H^+, Ca-montmorillonite, en, Cu(II). The species are plotted in % of L_0 = (total en) *vs.* −log h. Calculations were performed with the aid of GRFIT (Ludwig, 1992) for A) L_0 = 0.0001 mol/dm³, B) L_0 = 0.0002 mol/dm³, C) L_0 = 0.0005 mol/dm³, and D) L_0 = 0.0010 mol/dm³. C_0 was held constant at 0.0005 mol/dm³.

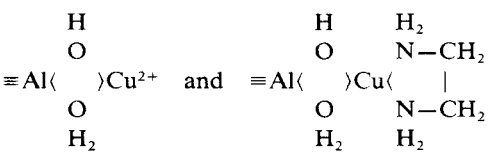

and

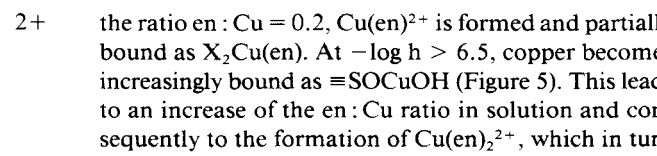

Using Eq. 20, Eq. 22 and the stability constant $K_{\equiv SOHCu^{2+}}$ as defined in Table 2a, a value of Q_1 = 10.2 is obtained.

As seen in Figure 4B, addition of en promotes copper adsorption in the region 4 < −log h < 6 and results in a partial desorption of copper in the range 7 < −log h < 9. The reason for this ambivalent behavior can be seen from the speciation diagrams for copper in Figure 5. In the range of 4 < −log h < 6 the onset of formation of $Cu(en)^{2+}$ species and their preference by the interlayer leads to an enhanced uptake of copper. In the region of 7 < −log h < 9, the formation of dissolved copper-en complexes prevents copper adsorption by surface hydroxyl groups. In this −log h range, the complete uptake of $Cu(en)_2$ by ion-exchange is impeded by the high Ca^{2+} concentration.

The obviously complicated effect of the increasing en_0 concentration upon the en uptake (Figure 4A) is clarified by the speciation diagram of en (Figure 6). For the ratio en : Cu = 0.2, $Cu(en)^{2+}$ is formed and partially bound as $X_2Cu(en)$. At −log h > 6.5, copper becomes increasingly bound as ≡SOCuOH (Figure 5). This leads to an increase of the en : Cu ratio in solution and consequently to the formation of $Cu(en)_2^{2+}$, which in turn results in a formation of $X_2Cu(en)_2$. At higher en : Cu ratios, the species $X_2Cu(en)_2$ and $X_2Cu(en)_3$ are chiefly responsible for the en uptake above −log h = 5.

Ternary surface complexes were found, in both the en and the copper speciation, to be of minor importance, influencing markedly the en adsorption only at low en : Cu ratios and in the range of −log h < 6.5.

The system β-alanine-copper-Ca-montmorillonite

The complexes of β-alanine and copper in solution are $Cu(\beta\text{-ala})^+$ and $Cu(\beta\text{-ala})_2$ existing in the range of 3.0 < −log h < 8.5 and −log h > 4, respectively. The experimental data of copper adsorption as presented in Figure 7B reflect clearly the influence of β-alanine competition in solution: The amount of copper bound by Ca-montmorillonite is decreasing with increasing ligand concentration. Copper adsorption at very low Cu : β-ala ratios (1:8) in the range of 4.5 < −log h < 7 is found to be underestimated by a model including only ligand competition in solution, which can be taken as an indication of a weak ternary complex.

https://doi.org/10.1346/CCMN.1994.0420205 Published online by Cambridge University Press

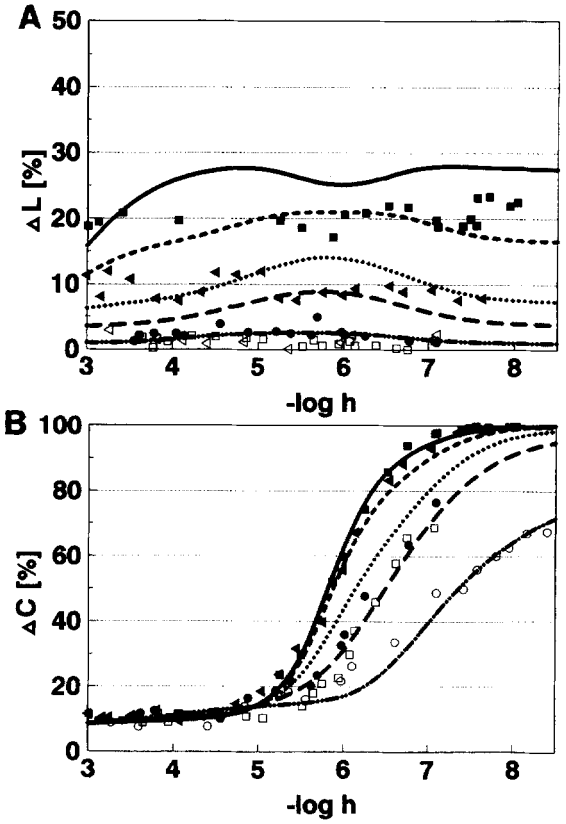

Figure 7. A) Sorption of β-ala on Ca-montmorillonite in the presence of Cu(II) (C_0 = 0.0005 mol/dm³, I = 0.3, T = 298.2 K). The percentage of sorbed ligand, ΔL, is plotted against −log h. Symbols indicate experimental data for L_0 = 0.0001 mol/dm³ (■), L_0 = 0.0002 mol/dm³ (▲), L_0 = 0.0005 mol/dm³ (●), L_0 = 0.0010 mol/dm³ (□), and L_0 = 0.0040 mol/dm³ (△). Lines indicate calculated curves for L_0 = 0.0001 mol/dm³ (——), L_0 = 0.0002 mol/dm³ (-----), L_0 = 0.0005 mol/dm³ (·····), L_0 = 0.0010 mol/dm³ (– – –), and L_0 = 0.0040 mol/dm³ (-·-·-). The curves were calculated with the stability constants given in Tables 2 and 3. B) Sorption of copper on Ca-montmorillonite in the presence of β-ala. (C_0 = 0.0005 mol/dm³, I = 0.3, T = 298.2 K). The percentage of adsorbed Cu(II), ΔC, is plotted against −log h. Symbols indicate experimental data for L_0 = 0.0001 mol/dm³ (■), L_0 = 0.0002 mol/dm³ (▲), L_0 = 0.0005 mol/dm³ (●), L_0 = 0.0010 mol/dm³ (□), and L_0 = 0.0040 mol/dm³ (○). Lines indicate calculated curves for L_0 = 0.0001 mol/dm³ (——), L_0 = 0.0002 mol/dm³ (-----), L_0 = 0.0005 mol/dm³ (·····), L_0 = 0.0010 mol/dm³ (– – –), and L_0 = 0.0040 mol/dm³ (-·-·-). The curves were calculated with the stability constants given in Tables 2 and 3.

Several assumptions were made and tested in model runs. Finally, the ion-exchange reaction:

$$Cu^{2+} + \beta\text{-ala}^- + X^- \Leftrightarrow Cu(\beta\text{-ala})X$$

$$K_{30} = \frac{[Cu(\beta\text{-ala})X]}{[Cu^{2+}]\cdot[\beta\text{-ala}^-]\cdot[X^-]} \qquad (30)$$

was found to improve the model. In addition, the stability constants of Cu(II)-(β-ala) complexes in solution were included into the optimization procedure. The

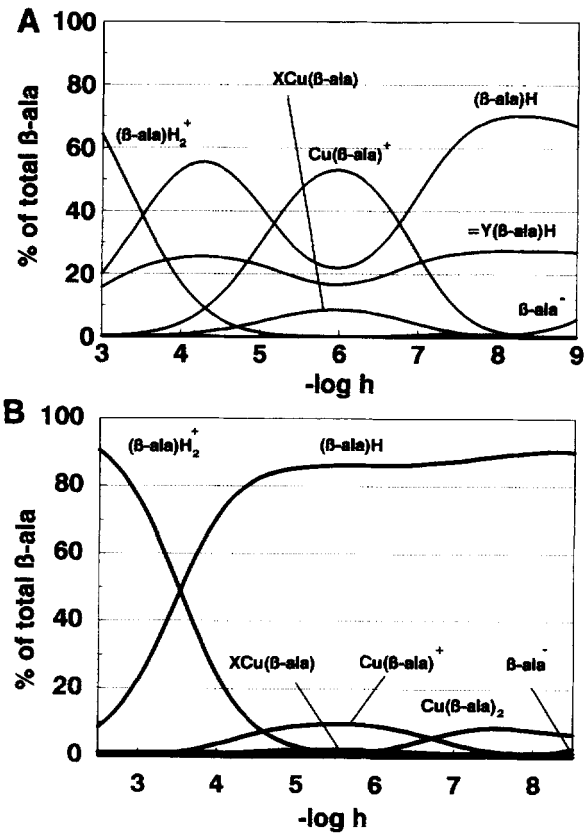

Figure 8. Speciation of β-ala in the system H^+, Ca-montmorillonite, β-ala, Cu(II). The species are plotted in % of L_0 (total β-ala) *vs.* −log h. Calculations were performed with the aid of GRFIT (Ludwig, 1992) for A) L_0 = 0.0001 mol/dm³ and B) L_0 = 0.0040 mol/dm³. C_0 was held constant at 0.0005 mol/dm³.

obtained stability constants are listed in Tables 2b and 3. Calculated model curves are shown in Figures 7A and 7B.

Reaction 30 takes place in the range of 3.5 < −log h < 8.5 and can, therefore, be used as an explanation for the observed enhanced copper adsorption in this −log h region (Figure 7B). On the other hand, the presence of copper has a weak effect on the adsorption of β-alanine (Figure 7A): Due to complexation in solution, the amount of β-alanine being sorbed on the surface is reduced without changing the general behavior of this ligand towards Ca-montmorillonite. The uptake of the 1:1 copper-β-alanine complex by ion-exchange is reported by Tsunashima (1984). As can be seen from both the β-alanine and the copper speciation (Figures 8 and 9, respectively), Cu(β-ala)X plays a very minor role for all investigated Cu : (β-ala) ratios.

The ternary system malonate-copper-Ca-montmorillonite

In solution, Cu^{2+} and malonate form the complexes Cu(mal) and $Cu(mal)_2^{2-}$. Under the experimental con-

https://doi.org/10.1346/CCMN.1994.0420205 Published online by Cambridge University Press

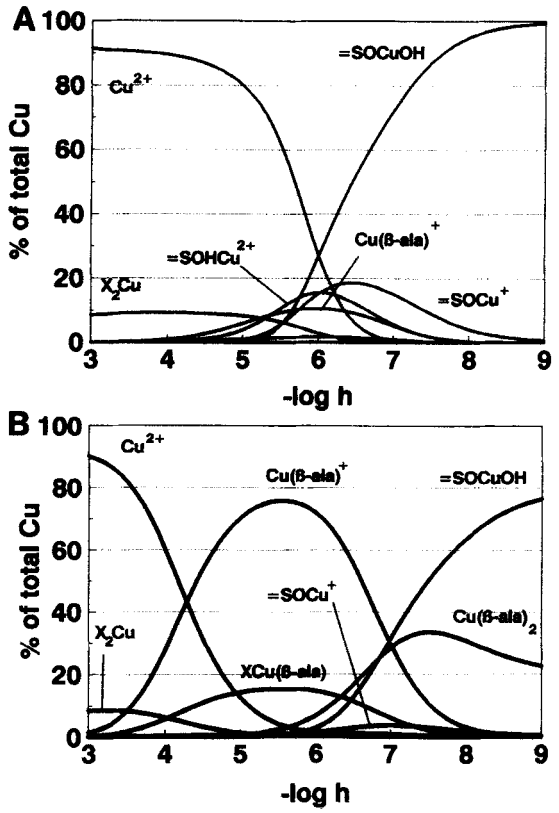

Figure 9. Speciation of Cu(II) in the system H^+, Ca-montmorillonite, β-ala, Cu(II). The species are plotted in % of C_0 (total Cu(II)) *vs.* −log h. Calculations were performed with the aid of GRFIT (Ludwig, 1992) for A) L_0 = 0.0001 mol/dm³ and B) L_0 = 0.0040 mol/dm³. C_0 was held constant at 0.0005 mol/dm³.

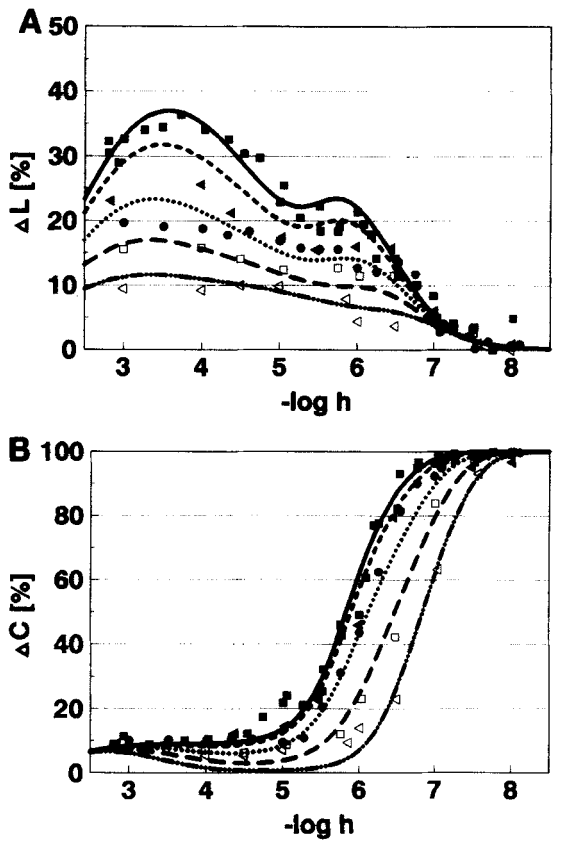

Figure 10. A) Sorption of mal on Ca-montmorillonite in the presence of Cu(II) (C_0 = 0.0005 mol/dm³, I = 0.3, T = 298.2 K). The percentage of adsorbed ligand, ΔL, is plotted against −log h. Symbols indicate experimental data for L_0 = 0.0001 mol/dm³ (■), L_0 = 0.0002 mol/dm³ (▲), L_0 = 0.0005 mol/dm³ (●), L_0 = 0.0010 mol/dm³ (□), and L_0 = 0.0020 mol/dm³ (△). Lines indicate calculated curves for L_0 = 0.0001 mol/dm³ (——), L_0 = 0.0002 mol/dm³ (- - - -), L_0 = 0.0005 mol/dm³ (· · · · ·), L_0 = 0.0010 mol/dm³ (– – –), and L_0 = 0.0020 mol/dm³ (–·–·–). The curves were calculated with the stability constants given in Tables 2 and 3. B) Sorption of Cu(II) on Ca-montmorillonite in the presence of mal (C_0 = 0.0005 mol/dm³, I = 0.3, T = 298.2 K). The percentage of adsorbed Cu(II), ΔC, is plotted against −log h. Symbols indicate experimental data for L_0 = 0.0001 mol/dm³ (■), L_0 = 0.0002 mol/dm³ (▲), L_0 = 0.0005 mol/dm³ (●), L_0 = 0.0010 mol/dm³ (□), and L_0 = 0.0020 mol/dm³ (△). Lines indicate calculated curves for L_0 = 0.0001 mol/dm³ (——), L_0 = 0.0002 mol/dm³ (- - - -), L_0 = 0.0005 mol/dm³ (· · · · ·), L_0 = 0.0010 mol/dm³ (– – –), and L_0 = 0.0020 mol/dm³ (–·–·–). The curves were calculated with the stability constants given in Tables 2 and 3.

ditions chosen in this study, the formation of these dissolved species is already important at −log h = 3. As visualized in Figure 10B, addition of malonate leads to a parallel shift of copper adsorption (involving ≡SOH groups) to higher −log h values; the extent of this shift increases with increasing ligand concentration. This shift reflects competition between surface ligand (≡SOH sites) and dissolved ligand. On the other hand, the formation of copper-malonate complexes in solution decreases the concentration of adsorbable malonate ions. Comparison of Figures 3A and 10A shows that the percentage of adsorbed ligand decreases with increasing copper concentration. An interesting feature of Figure 10A is the occurrence of a second adsorption maximum in the region of 5.5 < −log h < 6.5, i.e., in the range where copper complexing by surface hydroxyl groups takes place. This suggests formation of ternary complexes according to the general equation

$$\equiv SOH + Cu^{2+} + mal^{2-} \Leftrightarrow \equiv SOH_xCu(mal)^{(x-1)+} + (1 - x)H^+ \quad (31)$$

From various test runs, it was seen that the principal species forms according to:

$$\equiv SOH + Cu^{2+} + mal^{2-} \Leftrightarrow \equiv SOCu(mal)^- + H^+$$

$$K_{32} = \frac{[\equiv SOCu(mal)^-]\cdot[H^+]}{[\equiv SOH]\cdot[Cu^{2+}]\cdot[mal^{2-}]} \quad (32)$$

https://doi.org/10.1346/CCMN.1994.0420205 Published online by Cambridge University Press

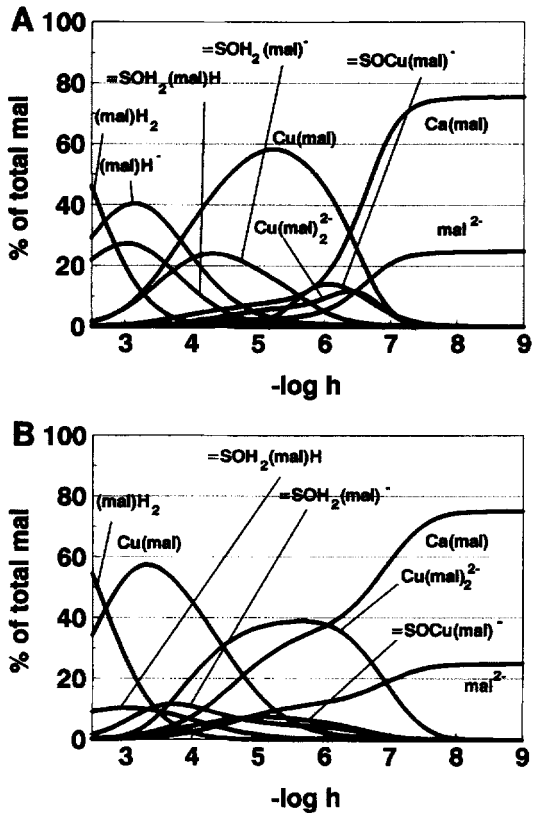

Figure 11. Speciation of mal in the system H^+, Ca-montmorillonite, mal, Cu(II). The species are plotted in % of L_0 = (total mal) *vs.* −log h. Calculations were performed with the aid of GRFIT (Ludwig, 1992) for A) L_0 = 0.0001 mol/dm³ and B) L_0 = 0.0020 mol/dm³. C_0 was held constant at 0.0005 mol/dm³.

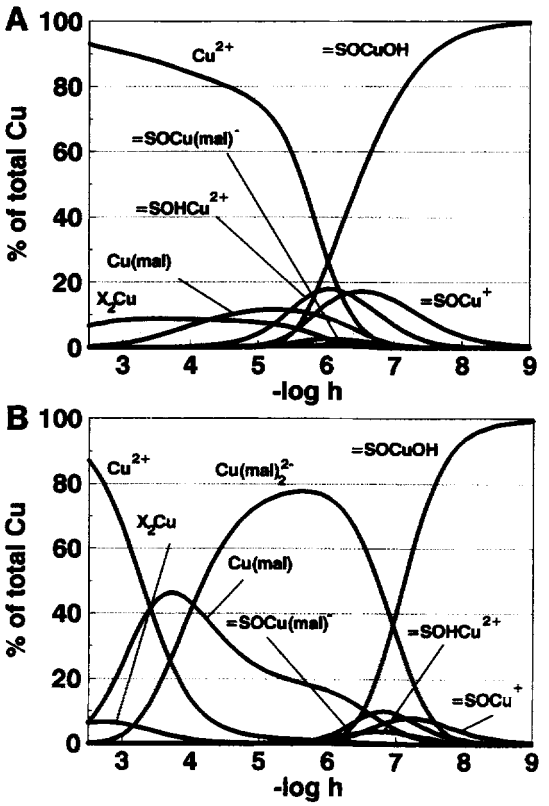

Figure 12. Speciation of Cu(II) in the system H^+, Ca-montmorillonite, mal, Cu(II). The species are plotted in % of C_0 (total Cu(II)) *vs.* −log h. Calculations were performed with the aid of GRFIT (Ludwig, 1992) for A) L_0 = 0.0001 mol/dm³ and B) L_0 = 0.0020 mol/dm³. C_0 was held constant at 0.0005 mol/dm³.

In addition, some evidence was found for the existence of one minor species:

$$\equiv SOH + Cu^{2+} + mal^{2-} \Leftrightarrow \equiv SOHCu(mal)$$

$$K_{33} = \frac{[\equiv SOHCu(mal)]}{[\equiv SOH]\cdot[Cu^{2+}]\cdot[mal^{2-}]} \qquad (33)$$

Including ≡SOHCu(mal) in the model resulted in a weak but significant improvement of the fit.

The proposed model is in fair agreement with the experimental data, as can be seen in Figures 10A (mal adsorption) and 10B (copper adsorption). As already pointed out in the discussion of the copper-en system, statistical effects (Schindler, 1990) predict a decrease of the stability constant by a factor of 12. The quotients Q_2 and Q_3 can be formed according to:

$$Q_2 = \frac{K_{\equiv SOCu^+}}{K_{\equiv SOCu(mal)^-}} = \frac{K_{\equiv SOCu^+}\cdot K_{Cu(mal)}}{K_{32}} = 17.8$$

$$Q_3 = \frac{K_{\equiv SOHCu^{2+}}}{K_{\equiv SOHCu(mal)}} = \frac{K_{\equiv SOHCu^{2+}}\cdot K_{Cu(mal)}}{K_{33}} = 29.5$$

where $K_{Cu(mal)}$ denotes the formation constant of the copper-malonate 1:1 complex in solution and $K_{\equiv SOHCu^{2+}}$ and $K_{\equiv SOCu^+}$ are taken from Table 2a. It can be seen that the stability of the principal ternary surface complex $\equiv SOCu(mal)^-$ is in fairly good agreement with statistical predictions, whereas the less important species ≡SOHCu(mal) is somewhat weaker.

In Figure 11, the speciation of mal is plotted for two Cu : mal ratios. It can be seen that for a Cu : mal ratio of 5:1, the proposed ternary surface complex $\equiv SOCu(mal)^-$ would be the most important surface species at $-\log h > 5.5$. For a Cu : mal ratio of 1:4, $\equiv SOCu(mal)^-$ would already dominate at $-\log h \geq 5$. The second ternary complex (≡SOCu(mal)H) is predicted to be never present in noticeable amounts. Figure 12 shows the speciation of copper. At high Cu : mal ratios (5:1), the copper speciation is clearly dominated by Cu^{2+} and the surface complex ≡SOCuOH. Lowering the Cu : mal ratio down to 1:4 results in a predominance of dissolved Cu(mal) and $Cu(mal)_2^{2-}$ complexes in the range of $3.5 < -\log h < 7$. The model anticipates the ternary

https://doi.org/10.1346/CCMN.1994.0420205 Published online by Cambridge University Press

surface complex ≡SOCu(mal)$^-$ to exist in noteworthy amounts in the region of $6 < -\log h < 8$.

CONCLUSION

The uptake of copper ions by Ca-montmorillonite is markedly influenced by the presence of chelate forming organic ligands. The three ligands investigated in this paper exemplify all possible modes of interaction that were described in the introduction. The presence of β-alanine tends to inhibit the adsorption of copper by ligand competition; however, a small contribution from ion-exchange by XCu(β-ala) was noticed. The presence of malonate shifts the range of copper uptake by surface hydroxyl groups towards alkaline regions. The effect is based on both ligand competition combined with the formation of ternary surface complexes. The addition of en promotes copper uptake in the acidic region by stabilizing the cationic species $Cu(en)_x^{2+}$ in the ion-exchanger. In the alkaline region ligand competition clearly reduces the percentage of adsorbed copper. The three above-mentioned mechanisms control in turn the influence of copper upon the extent of ligand uptake by Ca-montmorillonite. Ligand competition (β-alanine, Figure 7) tends to reduce the ligand uptake, whereas the formation of ternary surface complexes (malonic acid, Figure 10A, in the range of $5 < -\log h < 7$) enhances ligand adsorption. Enhanced ligand adsorption is finally also induced in cases where the metal-ligand complex is stabilized in the interlayer region of the clay mineral (en, Figure 4A). The different behavior of the three ligands is based on both the nature of the ligand atoms (N or O) and the charge of the ligand. The two factors are indeed coupled with each other. Copper(II) clearly prefers N-ligands as compared with O-ligands (Table 2b). Hence, ligand competition is more important for N-ligands than for O-ligands. This effect is, however, cancelled in part by the fact that proton affinity towards the ligand atoms shows the same trend. The main effect can be ascribed merely to the charge of the ligand: Ligands that form cationic complexes may assist ion-exchange. Ligands that form uncharged or negatively charged complexes are expected to participate in the formation of ternary surface complexes since the corresponding binary copper-clay surface complexes are formed in a $-\log h$ range where the charge of the binary copper-clay complex is positive. This effect can be recognized for the case of malonate.

ACKNOWLEDGMENTS

We thank Dr. C. Ludwig for putting the program GRFIT at our disposal, Mr. B. Trusch for technical assistance, and Dr. L. Marquis for valuable discussion. We are also grateful to Professor R. Giovanoli for the X-ray analyses and to Professor S. Sjöberg and Dr. R. Judd for reading and correcting the manuscript. This work was financially supported by the Swiss National Foundation.

REFERENCES

Benson, L. V. (1982) A tabulation and evaluation of ion exchange data on smectites: *Environ. Geol.* **4,** p. 23.

Bjerrum, N. (1948) *Bull. Soc. Chim. Belges* **57,** p. 432.

Bodenheimer, W., Heller, L., Kirson, B., and Yariv, S. (1962) Organo-metallic clay complexes. Part II: *Clay Miner. Bull.* **5,** p. 145.

Bodenheimer, W., Kirson, B., and Yariv, S. (1963) Organo-metallic clay complexes. Part I: *Israel J. Chem.* **1,** p. 69.

Bodenheimer, W., Heller, L., and Yariv, S. (1966) Organo-metallic clay complexes. Part VII: Thermal analysis of montmorillonite-diamine and glycol complexes: *Clay Miner.* **6,** p. 167.

Cloos, P. and Laura, R. D. (1972) Adsorption of ethylenediamine (EDA) on montmorillonite saturated with different cations. II. Hydrogen- and ethylenediammonium-montmorillonite protonation and hydrogen bonding: *Clays & Clay Minerals* **20,** p. 259.

Fletcher, P. and Sposito, G. (1989) The chemical modeling of clay/electrolyte interactions for montmorillonite: *Clay Miner.* **24,** p. 375.

Maes, A., Peigneur, P., and Cremers, A. (1978) Stability of metal uncharged ligand complexes in ion exchangers. Part 2. The copper+ethylenediamine complex in montmorillonite and sulphonic acid resin: *J. Chem. Soc. Faraday Trans. I* **74,** p. 182.

Martell, A. E. and Smith, R. M. (1976) *Critical Stability Constants:* Plenum Press, New York and London, 140 pp.

Shaviv, A. and Mattigod, S. V. (1985) Cation exchange equilibria in soils expressed as cation-ligand complex formation: *Soil Sci. Soc. Amer. J.* **49,** p. 569.

Siffert, B. and Espinasse, P. (1980) Adsorption of organic diacids and sodium polyacrylate onto montmorillonite: *Clays & Clay Minerals* **28,** p. 381.

Sillèn, L. G. and Martell, A. E. (1964) *Stability Constants of Metal-Ion Complexes, Section I: Inorganic Ligands:* The Chemical Society, London, Special Publication No. 17, 125 pp.

Schindler, P. W. (1990) *Co-adsorption of Metal Ions and Organic Ligands: Formation of Ternary Surface Complexes: Mineral-Water Interface Geochemistry, Vol. 23,* M. F. Hochella and A. F. White, eds., Mineralogical Society of America, Washington, D.C., p. 281.

Schindler, P. W. and Stumm, W. (1987) The surface chemistry of oxides, hydroxides and oxide minerals: in *Aquatic Surface Chemistry,* W. Stumm, ed., Wiley Interscience, New York, p. 83.

Stadler, M. and Schindler, P. W. (1993) Modeling of H^+ and Cu^{2+} adsorption on Calcium-montmorillonite: *Clays & Clay Minerals* **41,** 288–298.

Tsunashima, A. and Hayashi, H. (1984) Adsorption of some amino acids by Ca-, Co-, and Cu-montmorillonite: *Rep. Res. Inst. Underground Resources, Min. Coll., Akita Univ.* **49,** p. 53.

Velghe, F., Schoonheydt, R. A., and Uytterhoeven, J. B. (1977) Spectroscopic characterization and thermal stability of copper(II) ethylenediamine complexes on solid surfaces. 2. montmorillonite: *J. Phys. Chem.* **81,** p. 1187.

Westall, J. C. (1982) *A Program for the Determination of Chemical Equilibrium Constants from Experimental Data: User's Guide version 1.2:* Oregon State University, Corvallis, Oregon.

(Received 29 March 1993; accepted 9 August 1993; Ms. 2356)